Regional Diurnal Variations of Precipitation Parameters Observed with Tropical Rainfall Measuring Mission (TRMM) Microwave Imager (TMI) and TRMM Precipitation Radar (PR)

*Fumie A. Furuzawa[1], Kenji Nakamura[1]
(1: Hydrospheric Atmospheric Research Center, Nagoya University)
* HyARC, Nagoya University, 464-8601, Furo-cho, Chikusa Nagoya, Japan. e-mail: akimoto@hyarc.nagoya-u.ac.jp

Abstract

We analyzed the TRMM PR and TMI data over the ocean, land and coastlines by using the global each-passage data for June 1998, December 1998 - February 1999 (DJF) and obtained some results as follows. The PR reveals that 1) rainfall with a low storm height over land is dominant in winter or from 6 LT to 14 LT. There exists a convective rain more frequently from 12 LT to 20 LT and a stratiform rain exists more frequently in winter and from 6 LT to 8 LT. 2) precipitation has many larger drops from 18 LT to 24 LT for both convective and stratiform rains over the ocean and land on June and for both convective and stratiform rains over land on DJF. The diurnal variation is small over the ocean on DJF. Moreover it has many larger drops at tropics and especially lower in winter midlatitude, regardless of over the ocean and land on June and DJF. Especially, small size of precipitation is dominant over Tibetan plateau and the Andes. 3) monthly rainfall amount is the maximum at 19 LT on June and 15 LT on DJF over land, though TMI shows that the time is delayed a few hours. Difference between PR and TMI diurnal variations of rainfall rate is appeared from 10 LT to 17 LT and TMI rainfall rate is smaller than PR at the period. This is probably due to frequently appeared convective rain and/or frequently appeared shallow rain, as shallow rains have smaller TMI rainfall rate than PR and convective rains have also smaller TMI rainfall rate. Moreover, this period is coincident with the period without many large rain drops. This may imply that the TMI underestimates the surface rainfall rate at the case of rainfall without many large drops. We will discuss about the relationship on characteristics of rainfall and rainfall rates derived from PR and TMI.

Keywords: TRMM satellite, Precipitation, Regional variation, Diurnal variation

1. Introduction

Satellite observations of precipitation from space can get continuous, simultaneous and global informations. These global observations of rainfall activities with satellites are important because measurements of rainfall all over the ocean or tropical forest can be hardly done by ground-based observations. The TRMM satellite can detect directly obscured precipitation under the clouds by using microwave more exactly than other infrared or optical satellites. TRMM satellite has two microwave sensors; a precipitation radar (PR) and a TRMM microwave imager (TMI). The PR is an active radar which can determine 3 dimensional structure of precipitation system and precipitation parameters such as rain type and storm height. The rain rate is derived from TMI brightness temperatures and PR radar reflectivities, separately. The rain estimation algorithms for the PR and TMI are described by Iguchi et al. (2000) and Kummerow et al. (2001), respectively.

By the regional variations and diurnal variations of various precipitation parameters or regional dependencies of the diurnal variation observed with the PR, and then, we tried to understand the difference between PR and TMI rainfall rates, especially the difference of diurnal variation.

2. Data and Analysis

We analyzed the Level-2 data of the TRMM PR and TMI data over the ocean, land and coastlines separately by using the global each-passage data for June 1998, December 1998 − February 1999 (DJF). Level-2 data include meteorological parameters, such as rainfall rate, storm height, freezing height, and rain type (convective/stratiform/others, warm-rain). These data were produced by the National Aeronautics and Space Administration (NASA) and the Japan Aerospace Exploration Agency (JAXA) at the standard products version 5. The global each-passage data of various parameters were converted into grid data with grid size of 0.2 degrees (longitude) × 0.2 degrees (latitude). We show the results of the statistical analysis.

3. Results

3.1. Storm Height and Convective/Stratiform Fraction

At first, we focus on the PR storm height and rain type, because the difference between TMI and PR rainfall rate is large at the case of deep or shallow rain over land or convective rain over all surface conditions (Furuzawa and Nakamura 2004). Figure 1 shows the fraction of number of rain events with each storm height over land and Fig. 2 shows the fraction of stratiform rain ratio over land. They reveal that rainfall with a low storm height over land is dominant in winter or from 6 LT to 14 LT. There exists a convective rain more frequently from 12 LT to 20 LT and a stratiform rain exists more frequently in winter and from 6 LT to 8 LT. Instead of the number of rain events, we used the rain amount for each storm height. The result has also the same tendency as these figures (not shown). These results are in June 1998. During DJF, the same tendency was obtained except for the reverse of characteristics in the north and south.

3.2. Drop Size Distribution

A Z-R relation depends on drop size distribution (DSD) of precipitation. When the relation is written by the fol-

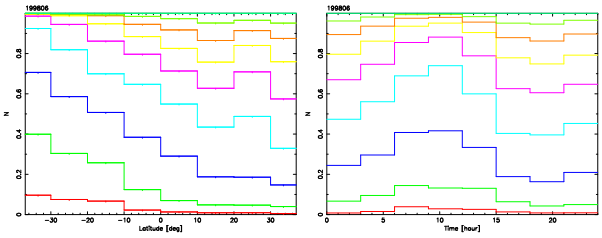

Fig. 1: Fraction of number of rain events with storm height, <3 km (between zero and the lowest red step line), 3 – 4 km (between the lowest red step line and a second lower green step line), 4 – 5 km, 5 – 6 km, 6 – 7 km, 7 – 8 km, 8 – 9 km, 9 – 10 km, and >10 km (between the highest chartreuse step line and unity) over land in June 1998. The left panel shows dependence on latitude, and the right one on local time every 3 hours. Cited from Furuzawa & Nakamura 2004.

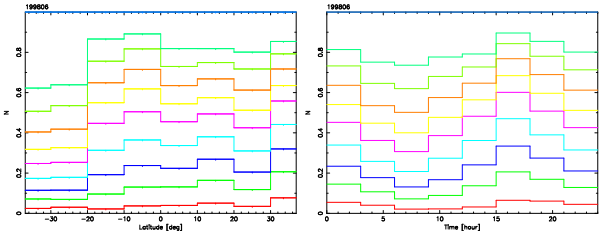

Fig. 2: Fraction of number of rainfall with each stratiform rain ratio, < 10 % (between zero and the lowest red step line), 10 – 20 % (between the lowest red step line and a second lower green step line), 20 – 30 %, 30 – 40 %, 40 – 50 %, 50 – 60 %, 60 – 70 %, 70 – 80 %, 80 – 90 %, and 90 – 100 % (between the highest chartreuse step line and unity) over land during June 1998. The left panel shows dependence on the latitude, and the right one shows on local time with every 3 hours. Cited from Furuzawa & Nakamura 2004.

lowing equation;

$$R = AZ^B, \tag{1}$$

two parameters, A and B, depend on DSD. It is known that the DSDs of each precipitation differ depending on rain type (Tokay and Short 1996, Iguchi et al. 2000, etc). We investigated the variation of Z-R relation for each region or latitude and for each local time on convective rain and stratiform rain, respectively. As cloud microphysical processes such as evaporation and collision rate, are functions of the DSD, DSD statistical studies can play an important role in cloud modeling studies. Those two parameters, A and B, were obtained by fitting all data of a PR reflectivity Z near the surface and PR rainfall rate R near the surface, within each grid with the size of 0.2° × 0.2° during one satellite passage, using the Z-R relation. These parameter values can be classified based on each hourly local time or each grid position. Figure 3 shows the diurnal variations of these parameters, for two rain types and for over the ocean and land. For all 8 cases, we can see the clear diurnal variations. These variations are similar with each other. During 10–17 LT, A-parameters are smaller than the mean values and B-parameters are larger. On the other hand, during 20–24 LT, A-parameters are larger and B-parameters are smaller. For convective rain, however, A-parameters are much larger than those for stratiform rain, and B-parameters are slightly smaller, as is well known (Tokay and Short 1996, Iguchi et al. 2000, etc). This means that the convective rain has no large rain drops. Moreover, for convective rain, the variations of both A-parameter and B-parameter over land are larger than those over the ocean, and their averaged values are larger. For stratiform rain, the same tendency is obtained for B-parameter. These results are for June 1998. During DJF, similar results are obtained except for over the ocean (not shown).

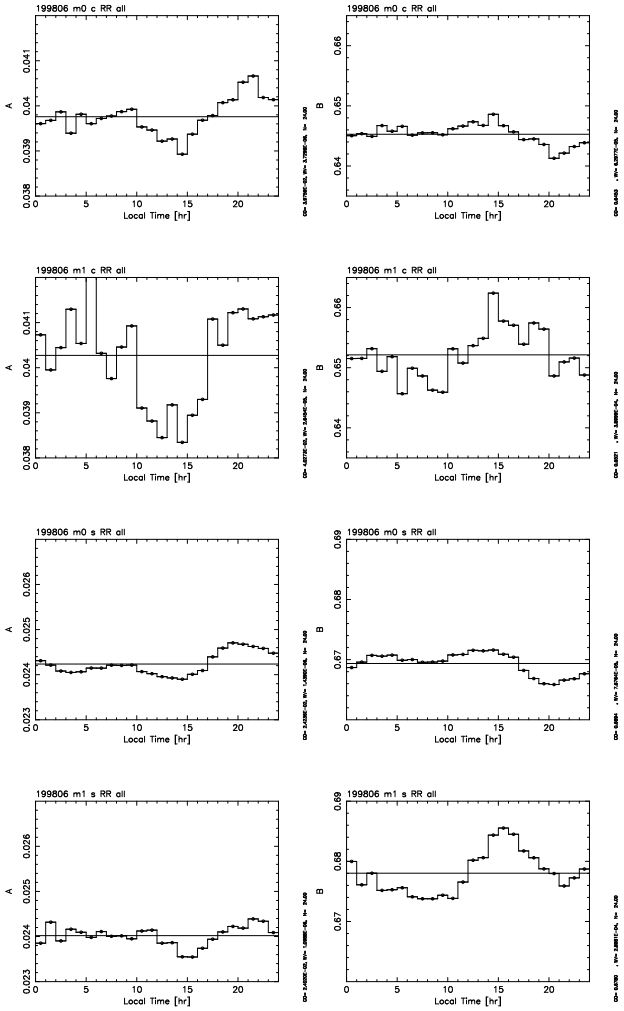

Fig. 3: Diurnal variations of A-parameter (left panels) and B-parameter (right panels) fitting Z-R relation in June 1998. Top 2 panels are for convective rain over the ocean, the next for convective rain over the land, the next for stratiform rain over the ocean, and bottom 2 panels are for stratiform rain over the land. Averaged values are shown by lines.

Relations between A-parameter and B-parameter for convective rain and stratiform rain are shown in Fig. 4. The larger A-parameter is, the smaller B-parameter is. It is consistent with the results of diurnal variations shown in Fig. 3. This tendency means that when A-parameter is large and B-parameter is small, that is, 20 – 24 LT, for strong rain, large drops are contained and Z is large, on the contrary, for weak rain, large drops are not contained and Z is small. On the other hand, when A-parameter is small and B-parameter is large, that is, 10 – 17 LT, for strong rain, large drops are not contained and Z is small, and for weak rain, large drops are contained and Z is large. Although the relation for stratiform rain is simple, that for convective rain has two streams. The inclination of the relation for stratiform rain is between two inclinations of

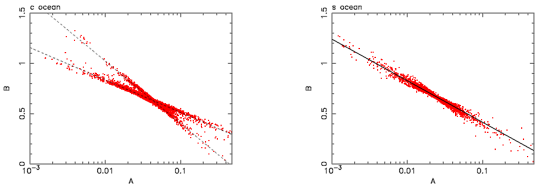

Fig. 4: Correlation between A-parameter and B-parameter fitting Z-R relation in June 1998. Left panel is for convective rain and right one is for stratiform rain. These are only over the ocean. The same tendency was obtained for over land. The best fitted model, $B \sim -0.4\log_{10}A$ is shown in right panel. In left one, two streams are shown by dotted lines, which are $B \sim -0.32\log_{10}A + 0.19, -0.62\log_{10}A - 0.22$.

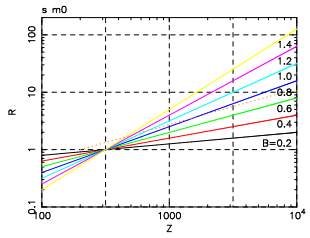

Fig. 5: Model Z-R relations, $Z = 316R^{1/B}$, obtained from the best fitting equation for stratiform rain over the ocean in June 1998, shown in right panel of Fig. 4. 7 cases for B-parameters of 0.2 – 1.4 are shown. All lines are through the point with 25 dBZ and 1 mm hr^{-1}. Orange dotted line is referred from Marshall & Palmer (1948), $Z = 200R^{1.60}$, representing for midlatitude stratiform condition. The NEXRAD relation; $Z = 300R^{1.40}$ is nearly equall with the result of B-parameter of 0.7 (not shown).

these streams for convective rain.

At the case of stratiform rain over the ocean, the relation between A-parameter and B-parameter are described by $B \sim -0.4\log_{10}A$ with deviation of $B < 0.1$. This means that the Z-R relation depends on only one parameter. We show the relation for various B-parameters of from 0.2 to 1.4 in Fig. 5. This figure indicates that critical rain rate, which is stated in the previous paragraph, is 1 mm hr^{-1}. Therefore, for almost all cases ($R > 1$ mm hr^{-1}), the previous statement for strong rain is valid. That is, at the case of small B-parameter (20 – 24 LT), large drops exist, on the contrary, and at the case of large B-parameter (10 – 17 LT), large drops do not exist.

In Fig. 6, we show the dependences of A-parameter and B-parameter on latitude for convective rain and stratiform rain over the ocean and land, respectively. Over the ocean, A-parameter is smaller and B-parameter is larger at midlatitude for both convective and stratiform rain. Especially, the tendency is remarkable at winter midlatitude.

To understand the global DSD map, we show the maps of A-parameter for convective rain and stratiform rain, respectively in Fig. 7. At first glance, A-parameter is low at winter midlatitude and A-parameter is very low over Tibetan plateau. These tendencies are seen for both convective rain and stratiform rain and are consistent with Fig. 6. We excluded the data over Tibetan plateau (70° <longitude < 110°) and checked the dependencies of A-parameter and B-parameter on latitude over land again. The results are shown in bottom two panels of Fig. 6. At the latitude of over 30°N, A-parameter increases and parameter-B also drastically decreases, for both convective and stratiform rain. These maps of Fig. 7 are for June 1998. In Fig. 8, we show the same maps for DJF. Parameter-A is also low at winter midlatitude and A-parameter is very low over Tibetan plateau and over around the Andes. Eventually, it is likely that large drops do not exist over Tibetan plateau, the Andes and at winter midlatitude.

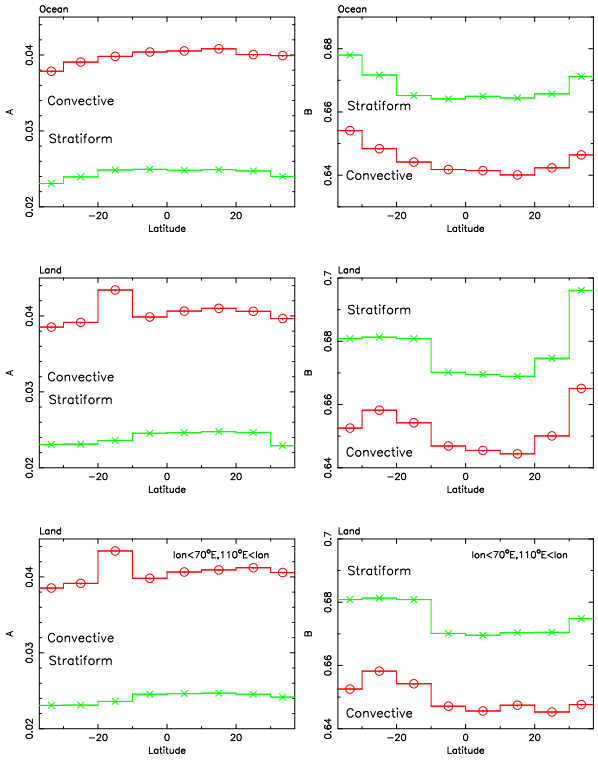

Fig. 6: Dependence of A-parameter (left panels) and B-parameter (right panels) fitting Z-R relation on latitude in June 1998. Top 2 panels are over the ocean, the other panels are over the land. Bottom 2 panels are for selected-longitude over the land. Red step lines and open circles are for convective rain, and green step lines and crosses are for stratiform rain, respectively.

3.3. Diurnal Variation of Rainfall Rate

TMI and PR observe a rain system nearly simultaneously, that is, within less than one minute due to the difference in the scan geometries. The quasi-simultaneous measurement gave us a significant opportunity to improve the rain intensity estimates by radiometers and rain radars. In Fig. 9, we show the difference of diurnal variation between TMI and PR over land. TMI rainfall rate is smaller than PR from 10 LT to 17 LT and larger than from 20 LT to 24 LT. Therefore, TMI diurnal variation looks delay a few hours. At least, TMI rainfall-maximum-time is observed to be delayed a few hours.

4. Discussion

The cause of differences between surface rainfall rates estimated by TMI and PR is thought to be TMI underestimate of rainfall rate for shallow rain over land due to lack of ice scattering or convective rain and TMI overestimation of deep rain due to evaporation or tilting system.

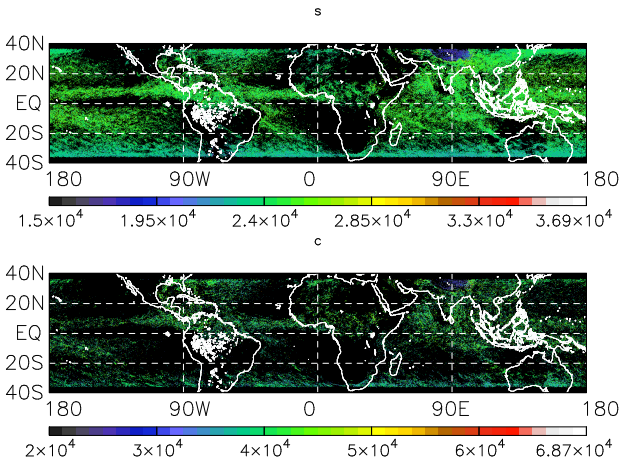

Fig. 7: Maps of A-parameter fitting Z-R relation for stratiform rain (top panel) and convective rain (bottom panel) in June 1998. Unit is 10^{-6}.

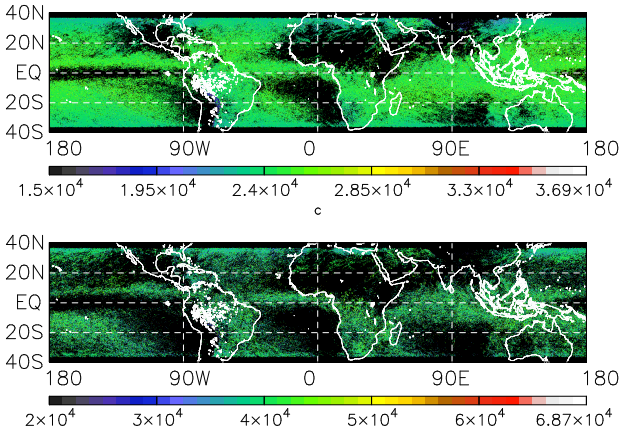

Fig. 8: Same as Fig. 7 but for DJF.

Moreover, over land, the period that TMI rainfall rate is smaller than PR (10 – 17 LT) is consistent with that large drops do not exist, and the period that TMI rainfall rate is larger (20 – 24 LT) is consistent with that large drops exist. This means TMI weakness for rain estimation of shallow rain or deep rain over land may be due to DSD.

At winter midlatitude, DSD variation is remarkable over the ocean, in addition to over-land case. On the other hand, the relation between TMI and PR rainfall rate over winter midlatitude is different from that over tropical region for both over-the-ocean case and over-land case. In Fig. 10, we show the scatter plots between TMI and PR rainfall rate for stratiform rain over the ocean. This figure shows that TMI rainfall rate is smaller than PR at strong rain, and TMI is larger than PR at weak rain at winter midlatitude. This tendency may be due to different DSD, that is, a Z-R relation with small A-parameter and large B-parameter, when there is no large drops for strong rain but weak rain has large drops. If so, in TMI estimation algorithm, the effect of DSD variation must be considered.

For convective rain, the relation between A-parameter and B-parameter has two streams. This may result in the TMI underestimation of rainfall rate.

5. Conclusions

We investigated the relationship between characteristics of rain system and surface rainfall rates estimated by TMI and PR by using the global each-passage instantaneous data.

The PR reveals that, at a period that a low storm height is dominant over land and larger drops do not exist or at a period that a convective rain is dominant, difference between PR and TMI diurnal variations of monthly rainfall rate happens due to TMI underestimation of rainfall rate. At a period that a deep rain is dominant over land and larger drops exist, the difference happens due to TMI over estimation. That is, uncertainty of TMI rainfall rate estimation probably depends on the drip size distribution, storm height and rain type.

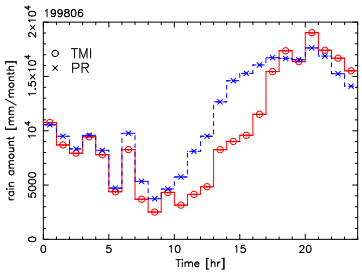

Fig. 9: Dependence of rain amount RT on local time over land in June 1998. Open circles show the TMI-RT, and crosses show the PR-RT. The TMI-RT is smaller than PR-RT in the day time and larger than PR-RT in the late evening. This means that the diurnal variation is different between PR and TMI. Cited from Furuzawa & Nakamura, 2004.

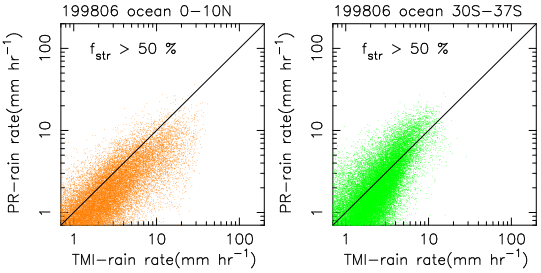

Fig. 10: Relation between TMI and PR rainfall rates for stratiform rain over the ocean in June 1998 at the latitude of 0 – 10°N (left) and 30°S – 37°S (right).

References

Furuzawa, A. F. and K. Nakamura, Differences of Rainfall Estimates over Land by Tropical Rainfall Measuring Mission (TRMM) Precipitation Radar (PR) and TRMM Microwave Imager (TMI) — Dependence on Storm Height. *J. Appl. Meteor.*, accepted, 2004.

Iguchi, T, T. Kozu, R. Meneghini, J. Awaka, and K. Okamoto, Rain-Profiling algorithm for the TRMM precipitation radar. *J. Appl. Meteor.*, **39**, 2038−2052, 2000.

Kummerow C., Y. Hong, W. S. Olson, S. Yang, R. F. Adler, J. McCollum, R. Ferraro, G. Petty, D.-B. Shin, and T. T. Wilheit, The evolution of the Goddard Profiling Algorithm (GPROF) for rainfall estimation from passive microwave sensors. *J. Appl. Meteor.*, **40**, 1801−1820, 2001.

Marshall, J. S, and W. M. Palmer, The Distribution of Raindrops with Size. *Journal of Meteorology*, **5**, 165−166, 1948.

Tokay A. and D. A. Short, Evidence from Tropical Raindrop Spectra of the Origin of Rain from Stratiform versus Convective Clouds. *J. Appl. Meteor.*, **35**, 355−371, 1996.